

Adsorption of Lead (II) from Aqueous Solution using Activated Carbon Prepared from Raffia Palm (*Raphia Hookeri*) Fruit Epicarp

Ghogomu, J. N¹, Muluh, S. N¹, Ajifack, D. L¹, Alongamo, A.A.B¹,
Noufame, D. T¹

¹(Department of Chemistry, Faculty of Science, University of Dschang, P.O. Box 6, Dschang, Cameroon)

Abstract: Activated carbons from raphia hookeri fruit epicarps obtained by chemical activation using ZnCl₂ (CAZn), H₃PO₄ (CAH) and KOH (CAK) were utilized for the removal of lead (II) ion from aqueous solution. Samples were characterized by FTIR, Boehm method, pH_{zpc}, iodine number, bulk density and surface area. Batch adsorption experiments were performed to study the effects of contact time, solution pH, adsorbent mass and initial adsorbate concentration at 27 °C. Optimal conditions from equilibrium studies were as follows: contact times of 80 minutes for CAZn and CAH and 100 minutes for CAK, pH = 6 for all samples, adsorption capacities of 66.37 mg/g for CAZn, 56.30 mg/g for CAH and 28.0 for CAK. Adsorption was modeled using Langmuir, Freundlich, Temkin and Dubinin-Radushkevich isotherm models. Equilibrium data were best represented by Langmuir isotherm model with monolayer adsorption capacities of 72.62 mg/g, 58.62 mg/g and 12.16 mg/g for CAZn, CAH and CAK respectively. Adsorption kinetics was via pseudo-first order, pseudo-second order, Elovich and intra-particle diffusion models. Kinetic studies revealed that the adsorption process followed pseudo-second order model. *Raphia hookeri* based activated carbons (CAZn and CAH) are shown to be promising materials for the adsorption of lead(II) ions from aqueous solutions.

Keywords: Activated carbon, Adsorption, Chemical activation, Lead (II) ions, *Raphia hookeri*.

I. Introduction

The problem of water contamination is neither new nor limited to a particular geographical area. Ecotoxicity specifically from wastewater contaminated with dyes, hydrocarbons and heavy metals from various manufacturing processes has become a serious environmental issue in recent years. Unlike organic pollutants, the majority of which are susceptible to biological degradation, these heavy metals do not degrade into harmless end products and their presence in streams and lakes leads to bioaccumulation in living organisms causing health problems in animals, plants, and human beings [1,2]. Lead (Pb), a heavy metal, has recently gained increasing attention owing to its high toxicity to living organisms [3]. Lead ions are taken into the body via inhalation, ingestion or skin absorption. Lead accumulates mainly in bones, brain, kidney and muscles and may cause many serious disorders like anaemia, kidney diseases etc. Lead is also known to cause mental retardation, reduces haemoglobin reproduction necessary for O₂ transport and it interferes with normal cellular metabolism. Lead equally has damaging effects on the body's reproductive and central nervous system [4]. As a result of these, environmental regulatory boards often spell out limitations as to the maximum concentration of lead in natural water and for wastewater discharge. The current U.S. Environmental Protection Agency (EPA) and World Health Organization (WHO) standard for lead in wastewater and drinking water is 0.5 and 0.05 mg/L, respectively [5]. Several treatment methods have been suggested, developed and used to remove heavy metals from wastewater, some of which include: chemical precipitation, ion exchange, membrane separation, complexation, adsorption, solvent extraction and distillation [6] are all geared towards greater amelioration of the quality of water/environment [7]. Amongst these methods, adsorption which is reported in this study has shown high potentials and simplicity in the depollution of industrial wastewater, especially in the elimination of lead [8]. Nevertheless, its efficiency depends largely on the adsorbent (cost, availability, and its regeneration) put together. The cost of preparing activated carbon from agricultural wastes is negligible when compared to the cost of commercial activated carbon. Present day researchers have utilized different low-cost materials as adsorbents which at times are less efficient. [9] prepared *militia ferruginea* plant leaves-based activated carbon for the sorption of Pb(II) ions in aqueous solution with a maximum adsorption capacity of about 3.3 mg/g of Pb(II) from a model based on the Freundlich adsorption isotherm. According to [10] maximum adsorption of Pb(II) ions by phosphoric acid activated carbon prepared from fluted pumpkin seed shell was of the order of 14.29 mg/g of adsorbent. In another study, [11], investigated on the adsorption performance of H₃PO₄ treated Nipa Palm Nut (NPN) based activated carbon for the uptake of Pb(II) and reported a monolayer adsorption capacity of 125 mg/g via the Langmuir model. On their own part, [12] showed that the maximum monolayer adsorption capacity of Pb(II) ions from aqueous solution using palm shell activated carbon was 13.4 mg/g. All these results show that

the adsorbents act as substitutes to commercial activated carbon in waste-water treatment. In the same vein, this study has been to evaluate the ability of chemically activated carbon prepared from *Raphia hookeri* fruit epicarps by zinc chloride, phosphoric acid and potassium hydroxide for the adsorption of Pb(II) from aqueous solutions.

II. Materials and Methods

2.1 Source and preparation of adsorbents

All the reagents and chemicals used were of analytical grade. The working solutions were prepared in distilled water. Raffia palm (*Raphia Hookeri*) fruit bunches were collected from fresh water swamp bushes of Pinyin Village in Santa Sub-Division, Mezam Division of the North West Region of Cameroon. The fruits were removed from the bunch, put in a plastic bag and left for a week. Thereafter, the epicarps were separated from the mesocarp and endocarp, washed and sun dried. The dried epicarps were then first crushed into smaller fragments with a mortar and pestle and later further ground into finer particles using an electric blender.

2.2 Chemical Activation and Pyrolysis

10 g sample of the precursor material was impregnated using either solutions of H₃PO₄, ZnCl₂ or KOH in a 1:1 (weight basis) impregnations ratio. The impregnation was carried out at 80 °C in a hot air oven for 24h to achieve well penetration of chemicals into the interior of the precursor material. The impregnated samples were then dried at 110 °C in an oven for 12h. The dried impregnated samples were transferred into porcelain crucibles with lids. Then the crucibles were placed inside an electric Muffle furnace and carbonized at 400 °C for 1h, in the absence of air. The carbonized samples were then cooled to room temperature and washed with 0.1 M hydrochloric acid (HCl) to remove the residual chemical agents followed by distilled water until the pH value of the rinsed water was neutral. The washed activated carbon was then dried in the oven at 110 °C for 5 hours. The samples were pulverized using a porcelain mortar and pestle and stored in an airtight bottle for later use. The adsorbents prepared by H₃PO₄, ZnCl₂ and KOH activations were denoted as CAH, CAZn and CAK respectively and the precursor material (biomass) denoted B throughout this study.

III. Characterization of Adsorbents

3.1 Analysis by Fourier-Transform-IR Spectrophotometer (FTIR)

In order to determine the surface functional groups existing on the samples, FTIR were carried out on samples using infrared spectrophotometer (Bruker alpha-p Spectrometer) with ethanol as solvent with a resolution of 4cm⁻¹ within the interval 400 - 4000 cm⁻¹.

3.2 Surface Function Determination by the Boehm Method

Titration of the total surface acidity and basicity of the activated carbons was carried out via the Boehm method [13]. In the determination of acidic surface functions (carboxylic, lactonic, phenolic), 40 mL each of decimolar solutions of NaHCO₃, Na₂CO₃, NaOH and HCl, were introduced into different reactors and each put in contact with 0.1 g of activated carbon sample. Titration of excess base was done by HCl solution. In the determination of the basic surface functions, 0.1 g of activated carbon was put in contact with 40 mL of a decimolar solution of HCl. After stirring for 48 hours, the excess acid was titrated with NaOH.

3.3 Iodine Number (IN)

The iodine number was measured according to the procedure established by the American Society for Testing and Materials (ASTM D2866-94), Iodine number is a relative indicator of porosity in an activated carbon. The iodine number is defined as the number of milligrams of iodine adsorbed by 1.0 g of carbon when the iodine concentration of the filtrate is 0.02 N. The iodine number is accepted as the most fundamental parameter used to characterize activated carbon performance. Iodine number was employed in this study as a test for microporosity via volumetric analysis. This fundamental test for the potentials of the prepared activated carbon determines its micro-porosity up to values as small as 2 nm. The iodine number is obtained from the following expression as described by [13]:

$$\text{Iodine number} = \frac{25.4 \times (30 - V_n)}{m_{AC}} \quad (1)$$

Where m_{AC} is the mass of activated carbon (g), V_n is the Volume of thiosulfate solution at equivalence point (mL).

3.4 Standardization of Iodine Solution

10 mL of 0.02 N iodine solutions were pipetted into a conical flask. 2-3 drops of starch solution were added. The pale yellow colour of iodine solution turned blue and was titrated with 0.005 N sodium thiosulphate till it became colourless.

3.5 Determination of pH at point of zero charge (pH_{pzc})

pH at point of zero charge, pH_{pzc}, corresponds to a pH at which the surface charge is nul. pH_{pzc} of the activated carbon samples were estimated according to standard procedure [13]. 50.0 mL of a decimolar solution of NaCl was introduced into reactors each containing 0.1 g of activated carbon to be analyzed. The pH of each solution was adjusted by addition of decimolar solutions of NaOH or HCl (by varying values of pH between 2 and 12). pH_{pzc} was determined by the intersection of the representative curves pH (final) = f[pH (initial)] and the first bisector curve. Stirring was maintained at 27 °C for 48 hours with the aid of a multi-agitator system (Edmund Bühler GmbH) shaking at 150 rpm. The contents of the reactors were then filtered with Whatman N°1 filter paper after which the pH of the final solutions was measured.

3.6 Bulk Density (g/cm³)

A measuring cylinder was weighed and then filled with the prepared activated carbon and gently tamped until no change in the level of the sample was observed. The volume occupied by the packed sample was recorded (V_s). If W_c is the weight of the empty cylinder and W the weight of the cylinder and dry sample, then weight of the dry sample W_s was obtained by [14]:

$$W_s = W - W_c \quad (2)$$

The bulk density (B_d) was calculated using [14]:

$$B_d \text{ (g/cm}^3\text{)} = \frac{\text{weight of dry Sample (g)}}{\text{Volume of packed dry sample}} \quad (3)$$

$$B_d \text{ (g/cm}^3\text{)} = \frac{W_s \text{ (g)}}{V_s \text{ (cm}^3\text{)}} \quad (4)$$

Where V_s is the volume occupied by the packed samples.

3.7 Surface Area

The diameter (assuming spherical shape) of the activated carbon was obtained by passing the crushed activated carbon through sieve size of 100 μm and the external surface area was calculated by the relation [14]:

$$\text{Surface area (m}^2\text{/g)} = \frac{6 \text{ (cm}^3\text{/g)}}{B_d \text{ (g/cm}^3\text{)} \cdot P_d} \quad (5)$$

where B_d is the bulk density and P_d is the particle size (particle diameter).

IV. Batch Adsorption Experiments

4.1 Preparation of Pb(II) Stock solution

The mother solution was prepared by dissolving 1.5985 g of Pb(NO₃)₂ inside a 1L volumetric flask with freshly prepared distilled water. Solutions of various concentrations used in the adsorption studies were obtained by diluting portions of the stock solution with distilled water.

4.2 Equilibrium Studies Using Batch Method

Equilibrium and kinetic adsorption experiments were carried out in a multi-agitator system (Edmund Bühler GmbH SM 30) maintained at 27 °C. All the experiments except the study of the effect of pH were carried out at a pH of 6. For each experiment, 0.5 g of adsorbent was measured and put into a 250 mL screw cap conical flask containing 20 mL of Pb(II) ions at the desired initial concentration which range from 100 - 700 mg/L in this study. After agitating the solutions for a predetermined time interval (20–160 minutes), samples were filtered using filter paper (Whatman N° 1). The filtered solution was put into test tubes containing dithizone and ammoniacal buffer solutions to form a complex. The concentration of the residual Pb(II) ions was determined spectrophotometrically using a UV-Vis Spectrophotometer (JENWAY) at λ_{max} = 490 nm. The quantity of Pb(II) ions adsorbed by a unit mass of adsorbent [Q_e(mg/g)] and the adsorption percentage (% Adsorption) at an instant was calculated from the difference between the concentrations of lead (II) before and after adsorption using the equations [15]:

$$Q_e = \frac{(C_o - C_e)V}{W} \quad (6)$$

$$\% \text{ Adsorption} = \frac{C_o - C_e}{C_o} \times 100 \quad (7)$$

V. Results and Discussions

5.1.1 Fourier Transform Infrared spectroscopy (FTIR)

In view of identifying the different functional groups and chromophores responsible for the various signals, the results obtained by Fourier Transform Infra-Red spectra analysis are presented in Figs. 1 and on Table 1. The FTIR spectra of the activated carbons pre-treated with different impregnation solutions are shown in Fig. 1. For the spectra of CAZn, CAH and CAK the reduction in the intensities of the broad band centred at 3334.64 cm^{-1} and the peak at 1030.71 cm^{-1} can be attributed to the disappearance of H_2O molecules after activation. It is equally observed that there is the disappearance of the peak at 2922.78 cm^{-1} after activation and carbonization due to the decomposition of some of the surface functions during pyrolysis.

Table 1: Interpretation of the IR spectrum of B

Absorption bands (cm^{-1})	Chromophores and functional groups
3600-3000	OH of carboxylic, phenols, alcohols, water
2928	CH of aromatic methoxyl groups
1698	C=O of ketones, aldehydes, lactones or of the carboxylic groups
1550-1650	carboxylic acid derivatives and amino acids.
1416	C=C bonds in the aromatic rings
1456-1420	CH_2 and/or O-H of carboxylic and phenol groups
1128 - 1168	C-O is characteristic of phosphorus and phosphorus-carbonated compounds of the phosphoric acid activated carbon.
1102	C-O of a secondary alcohol
526- 403	Para substitution of the benzene ring.
506	C-X bonds of halogeno alkanes

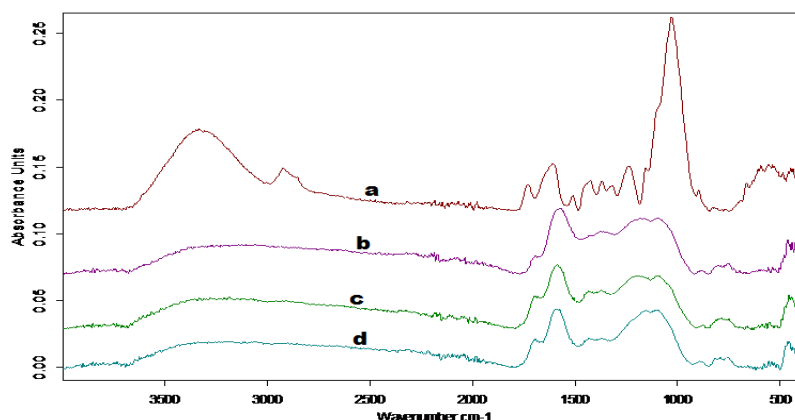


Figure 1: superposed FT-IR spectra of (a) biomass (B), (b) CAZn, (c) CAK and (d) CAH

5.2 Determination of oxygen containing functional groups

The results of the quantification of the surface acidic and basic functions of the activated carbon samples (CAZn, CAH and CAK) obtained via the Boehm method is presented on Table 2. Chemical analysis of the surface revealed that the samples contain more acidic (carboxylic and phenolic groups) than basic functions. This observation is coherent with the pH_{pzc} values obtained for each of the activated carbon samples.

Table 2: Quantification of surface oxygen-containing groups by the Boehm method

Samples	Carboxylic (meq/g)	Lactonic (meq/g)	Phenolic (meq/g)	Total acid (meq/g)	Total basic (meq/g)	Total (meq/g)
CAZn	0.431	0.0227	0.068	0.522	0.115	0.637
CAH	0.416	0.0134	0.041	0.470	0.053	0.523
CAK	0.381	0.0046	0.024	0.410	0.020	0.430

5.3 Iodine Number (IN)

Iodine number is a fundamental parameter used to determine the activity of activated carbons. It gives a better estimate of the amount of active surface present on the activated carbon. It is a measure of the micropore content of the activated carbon. The micropores are responsible for the large surface area of activated carbon particles and are created during the activation process [16]. The results of the Iodine Number obtained together with the bulk density and surface area values for the different adsorbents are presented in Table 3. From Table 3, the results suggest that CAZn with the largest iodine number has more micropores and thus a larger surface area than CAH and CAK.

Table 3: Iodine number, bulk density and surface area values for the different adsorbents

Adsorbent	Impregnation ratio	Bulk density (g/cm ³)	IN (mg/g)	Surface area(m ² /g)
CAZn	1:1	0.63	576.84	712.64
CAH	1:1	0.57	459.70	695.50
CAK	1:1	0.52	437.62	673.42

5.4 pH at point of zero charge (pHpzc)

The pH_{pzc} obtained for each activated carbon (Fig. 2) is coherent with the quantification of the surface functional groups obtained via the Boehm method. These pH_{pzc} values permit the determination of the acidic or basic character of the activated carbon and to know, according to the pH of the solution, the net surface charge. According to Fig. 2, it can be noticed that pH_{pzc} is 5.6, 5.0 and 5.2 respectively for CAZn, CAH and CAK. Hence, in experiments wherein pH_{pzc} > pH samples will have their surfaces positively charged while for those in which pH_{pzc} < pH will have their surfaces negatively charged.

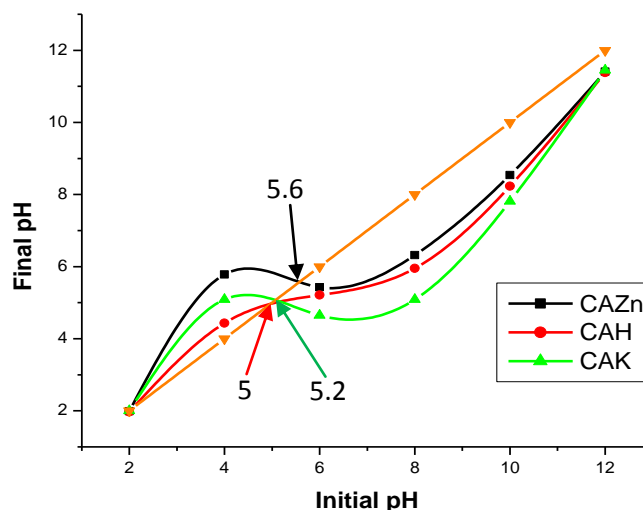


Figure 2: Graph for the pH_{pzc} for CAZn, CAH, CAK and B

5.5.1. Effect of pH

pH is one of the most important variables affecting the amount of heavy metal adsorbed by an adsorbent, because pH influences surface charge, degree of ionisation (protonation) of the functional groups on the adsorbent. The experiments were done under different pH values (between 2 and 8) keeping other parameters constant. The results are presented in Fig. 3. By increasing pH, increase in adsorption capacity of Pb(II) was observed and the maximum adsorption capacity was obtained at pH 6 corresponding to 72.62 mg/g, 58.62 mg/g, 12.16 mg/g and 10.94 mg/g (CAZn, CAH, CAK and B) respectively. Pb(II) adsorption decrease as pH rose beyond the optimum pH 6 because Pb²⁺ starts precipitating as Pb(OH)₂. At very low pH (pH < 3), low values of adsorbed Pb(II) ions were observed. This can be attributed to the facts that H⁺ ions concentration in solution is high, thus the functional groups on the adsorbent surface are protonated. Hence Pb(II) ion adsorption is low due to competition between the H⁺ and Pb²⁺ ions for free adsorption sites. The optimum pH of 6 was maintained in this study in subsequent parameter determinations.

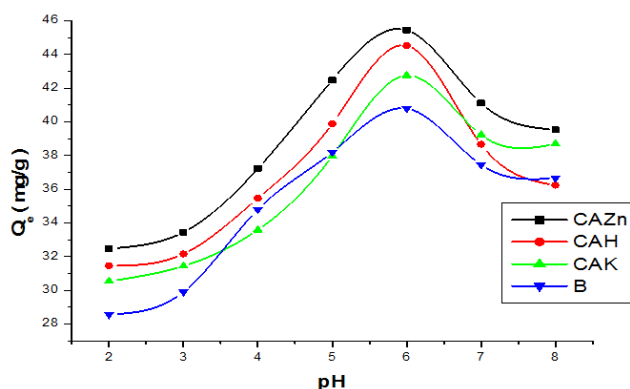


Figure 3: effect of pH on lead (II) ion adsorption onto CAZn, CAK, CAH and B. (C₀ = 100 ppm, adsorbent dose = 0.5 g, pH = 6, Contact time = 80 min, agitation speed = 150 rpm and T = 27 °C.)

5.5.1 Effect of Adsorbent dosage

The effect of adsorbent dose was determined at an initial metal ion concentration of 100 ppm and at pH 6. The results summarized in Fig. 4 indicate that, with an increase in mass of adsorbent in the range 0.1g to 1 g, adsorption capacity rapidly decreases. This effect can be due to some adsorption sites remaining unsaturated during the adsorption process. Low Pb(II) removal as adsorbent dose increased may be due to the fact that the adsorption of Pb(II) is limited by monolayer adsorption. This is corroborated by the value of the correlation coefficient, R^2 , from Langmuir isotherm.

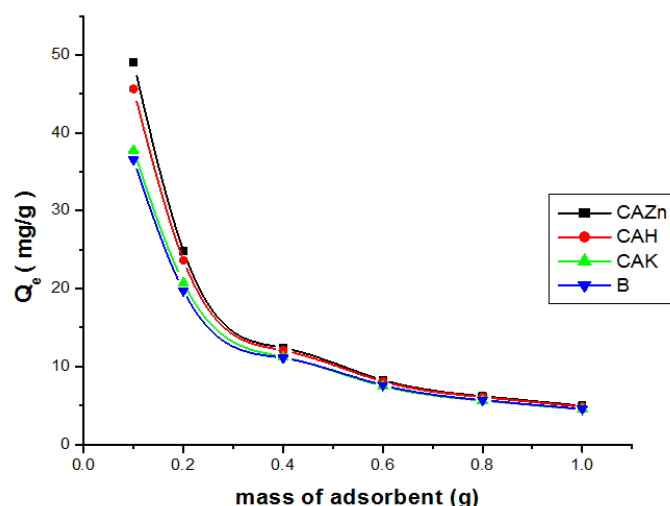


Figure. 4: Effect of adsorbent dose on the uptake of lead (II) ions onto CAZn, CAK, CAH and B. ($C_o = 100$ ppm, adsorbent dose = 0.5 g, pH = 6, Contact time = 80 min, agitation speed = 150 rpm and $T = 27$ °C.

5.5.2 Effects of Contact Time

The result of percentage Pb^{2+} adsorbed is shown in Figure 5. It was found that the amount of Pb^{2+} ions adsorbed increased with increasing contact time. It can be observed from the figure that a high rate of Pb^{2+} ions adsorption occurred in the first 20 to 60 mins for all the adsorbents and thereafter the rate of adsorption of the adsorbate species into the adsorbent was found to be slow. The time required to reach equilibrium on Pb^{2+} adsorption was 80 minutes for CAZn and CAH and 100 minutes for CAK. The initial rapid adsorption is due to the availability of the negatively charged surface of the adsorbents for adsorption of cationic Pb^{2+} species present in the solution. The later slow adsorption is probably due to the electrostatic hindrances between adsorbed positively charged adsorbate species into the surface of adsorbents and the available cationic adsorbate species in solution, and the slow pore diffusion of the solute ion into the bulk of the adsorbent [17].

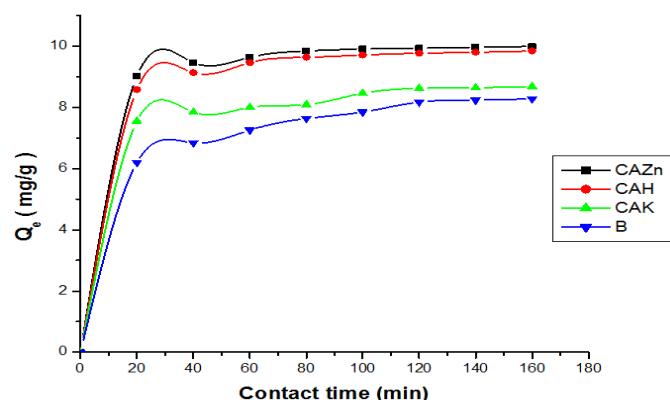


Figure 5: Effect of contact time on the adsorption of lead (II) onto CAZn, CAK, CAH and B. ($C_o = 100$ ppm, adsorbent dose = 0.5 g, pH = 6, Contact time = 80 min, agitation speed = 150 rpm and $T = 27$ °C

5.5 Effect of initial concentration of lead

The effect of initial Pb^{2+} ion concentration on the adsorption process was carried out with initial concentrations ranging from 100 to 700 ppm. The experimental results on the adsorption capacity are presented in Fig. 6. The result obtained show that an increase in the initial concentration leads to an increase in the quantity of Pb^{2+} ion adsorbed. However, the percentage adsorption decreased with increase in initial ion concentration.

The adsorption capacity of Pb^{2+} increase because increasing the initial concentration leads to an increase in the amount of Pb^{2+} ion in the solution resulting in an increase in collision between the molecules of the metals and the adsorption sites. With this increase in collision, the adsorption sites become more quickly saturated. Thus, at higher Pb^{2+} concentrations, the available adsorption sites become fewer and hence the adsorption of Pb^{2+} becomes more or less constant.

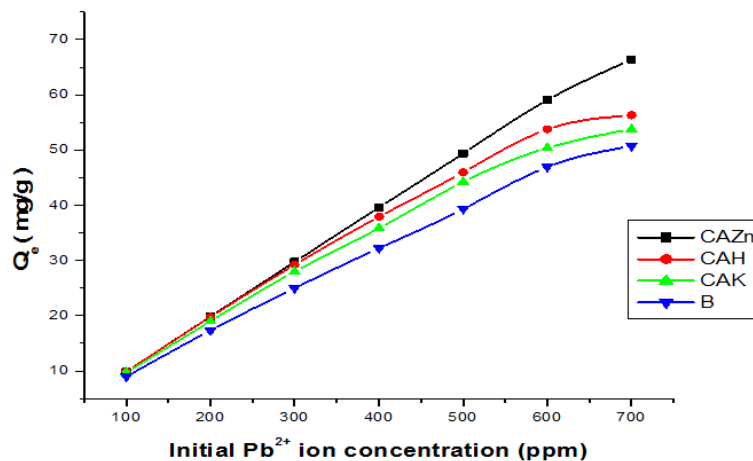


Figure 6. : effect of initial concentration on lead (II) adsorption on CAK, CAZn, CAH and B. ($C_o = 100$ ppm, adsorbent dose = 0.5 g, pH = 6, Contact time = 80 min, agitation speed = 150 rpm and $T = 27$ °C

5.6.1 Adsorption isotherm models

Adsorption isotherms are models used to characterize the relationship between the adsorbent (solid) and the adsorbate (solute), and knowledge of the adsorption capacity of the adsorbent can be described by several isotherm models such as Langmuir, Freundlich, Temkin and Dubinin-Radushkevich (D-R) models [18].

5.7.1 Langmuir adsorption isotherm

The Langmuir model assumes that the uptake of metal ions occurs on a homogeneous surface by monolayer adsorption without any interaction between adsorbed ions, that uniform energies of adsorption are involved, and that there is no transmigration of adsorbate in the plane of the surface [19]. The linearized Langmuir isotherm equation can be expressed as:

$$\frac{C_e}{Q_e} = \frac{K_L}{Q_m} + \frac{C_e}{Q_m} \quad (8)$$

Where, K_L is the Langmuir adsorption constant (L/mg) which is related to the maximum sorption capacity and energy of adsorption, C_e is the equilibrium concentration (mg/L), Q_e is the amount adsorbed per amount of adsorbent at equilibrium (mg/g) and Q_m (mg/g) is an indicator of monolayer adsorption capacity. The efficiency of the Langmuir adsorption process is further assessed by (9):

$$R_L = \frac{1}{1 + K_L C_o} \quad (9)$$

Where R_L is a dimensionless constant referred to as separation factor, K_L is the Langmuir constant related to the energy of adsorption and C_o is the initial solute concentration (mg/L). If $R_L > 1$ adsorption is said to be unfavorable, $R_L = 1$ for linear adsorption, $0 < R_L < 1$ for favorable adsorption and $R_L = 0$ for irreversible adsorption.

5.8 Freundlich adsorption Isotherm

Freundlich model assumes that the uptake of metal ions occurs on a heterogeneous surface by monolayer adsorption [20]. The linearized relation (10) is given below:

$$\log Q_e = \log K_f + \frac{1}{n} \log C_e \quad (10)$$

Where: Q_e is the quantity of solute adsorbed at equilibrium (adsorption density: mg of adsorbate per g of adsorbent). C_e is the concentration of adsorbate at equilibrium, $1/n$ (mg/L) is the adsorption intensity or the

heterogeneity factor and K_f is the Freundlich constant related to the adsorption energy (mol^2/kJ^2). These last two constants are dependent of temperature and the nature of sorbent and sorbate.

5.9 Temkin adsorption isotherm.

It is expressed in linear form by the following relationship between the amount adsorbed, Q_e , and concentration in solution at equilibrium, C_e , [19]:

$$Q_e = \frac{RT}{b_T} \ln A_T + \frac{RT}{b_T} \ln C_e \quad (11)$$

Where, A_T (L/g) is the Temkin isotherm constant (equilibrium binding constant), B_T (J/mol) is a constant related to heat of sorption, R is the gas constant ($8.314 \text{ JK}^{-1} \cdot \text{mol}^{-1}$) and T is the absolute temperature (K). Similar to the Freundlich equation, the Temkin model takes into account the heterogeneity of the surface [19].

5.10 Dubinin-Radushkevich (D-R) Isotherm

The Dubinin-Radushkevich isotherm helps to determine the apparent energy of adsorption, the characteristic porosity of adsorbent towards the adsorbate and it does not assume a homogeneous surface or constant adsorption potential. This isotherm is generally expressed as follows [21]:

$$Q_e = Q_{\max} e^{-\beta \varepsilon^2} \quad (12)$$

Where, Q_e is the amount of adsorbate on the adsorbent at equilibrium (mg/g); Q_{\max} is the theoretical isotherm saturation capacity (mg/g); ε is the polanyi potential given as:

$$\varepsilon = RT \ln \left(1 + \frac{1}{C_e} \right) \quad (13)$$

β is a constant related to the mean free energy of adsorption per mole of the adsorbate adsorbed to the adsorbent (mol^2/kJ^2). The energy can be obtained using the following relationship:

$$E = \frac{1}{\sqrt{2\beta}} \quad (14)$$

The linear form of D-R equation is expressed as:

$$\ln(Q_e) = \ln(Q_{\max}) + \beta \varepsilon^2 \quad (15)$$

From the D-R isotherm, the magnitude of the mean free energy of adsorption shows if the adsorption process follows physisorption, ion exchange or chemisorption. [22], reported that the means free energy for physisorption $< 40 \text{ KJ/mol}$ and that for chemisorption $> 40 \text{ KJ/mol}$.

In order to find the most appropriate model for the lead adsorption, the data were fitted to each isotherm model. The parameters of the different models are presented on Table 4 and only the Langmuir isotherm model ($R^2 = 0.9969, 0.9961, 0.9937$ and 0.9831 for CAZn, CAH, CAK and B respectively) represented on Figure 7 best fitted the experimental data. The homogeneous monolayer adsorption capacity of Pb(II) ions at 27°C were found to be equal to 72.62 mg/g , 58.62 mg/g , 12.16 mg/g and 10.94 mg/g for CAZn, CAH, CAK and B samples respectively. The shape of the Langmuir isotherm was investigated by the dimensionless constant separation term (R_L). In this investigation the equilibrium parameter was found to be in the range $0 < R_L < 1$ as shown in Table 4. This indicated that the sorption process was very favorable and that the adsorbent employed exhibits good adsorption potentials. Temkin isotherm model predicts a uniform distribution of binding energies over the population of surface binding adsorption. The values of Temkin constants A_T and B_T as well as the correlation coefficients are listed in Table 4. the D-R isotherm predict that the apparent energy of adsorption (E) which stands at 78.09 kJ/mol , 81.64 kJ/mol , 89.80 kJ/mol and 82.76 kJ/mol respectively for CAZn, CAH, CAK and B were all greater than 40 kJ/mol meaning the mechanism of adsorption of Pb^{2+} on all the adsorbents was chemisorption in which strong chemical bonds are involved.

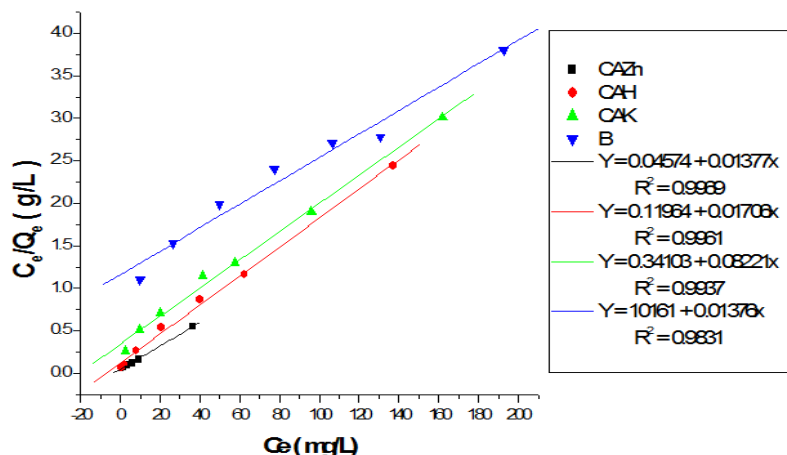


Figure 7: linear transformation of Langmuir isotherm

Table 4: Results of adsorption parameters for the different model isotherms

Models	Parameters	Adsorbents			
		CAZn	CAH	CAK	B
Langmuir	Q _o (mg/g)	72.62	58.62	12.16	10.94
	K _L (L/mg)	0.3010	0.1426	0.2411	0.079
	R ²	0.9969	0.9961	0.9937	0.9831
Freundlich	1/n	0.472	0.322	0.426	0.598
	n	2.119	3.106	2.347	1.672
	K _F (L/g)	17.233	13.625	7.150	2.387
	R ²	0.9701	0.734	0.9825	0.9817
Temkin	A _T (L/g)	3.309	3.827	0.706	0.144
	b _T (J/mg)	164.01	270.90	217.90	169.15
	B (kJ/mol)	15.106	9.146	11.370	14.647
	R ²	0.9781	0.9567	0.9563	0.9537
Dubinin-Radushkevich	Q _{max} (mg/g)	65.97	46.29	43.95	44.65
	β (mol ² /J ²)	0.82x10 ⁻⁴	0.75x10 ⁻⁴	0.62x10 ⁻⁴	0.73x10 ⁻⁴
	E (kJ/mol)	78.09	81.65	89.80	82.76
	R ²	0.9211	0.9198	0.8722	0.8894

5.11 Adsorption Kinetic Models

Several kinetic models are often used in modeling the adsorption mechanism of dissolved solutes on adsorbents. In this study, four kinetic models have been studied in describing the adsorption phenomenon of Pb (II) ions onto the two activated carbon samples studied herein: pseudo-first order, pseudo-second order, Elovich and intra-particle diffusion models.

5.12 Pseudo first-order model

In order to study the adsorption kinetics of Pb(II) ions, the kinetics parameters for the adsorption process were studied for contact times ranging from 20 to 160 min by monitoring the quantity of Pb(II) adsorbed as a function of time. The data were then regressed against the Lagergren equation (12), which represents a first order kinetics equation [23]:

$$\log(Q_e - Q_t) = \log Q_e + \frac{K_1}{2.303} t \quad (16)$$

where, k₁ is the pseudo-first-order rate constant (min⁻¹); Q_e and Q_t are the adsorption capacities at equilibrium and at a given time t expressed in (mg/g).

5.13 Pseudo second-order model

Represented by (17) below, the linearized pseudo-second order chemisorption kinetic model [23] has been frequently used in diverse experiments involving the adsorption of organics and heavy metals on activated carbon:

$$\frac{t}{Q_t} = \frac{1}{K_2 Q_e^2} + \frac{1}{Q_e} t \quad (17)$$

where, K₂ is the pseudo-second-order rate constant (mg.g⁻¹.min⁻¹).

5.14 Elovich model

The linearized Elovich equation is generally expressed as:

$$Q_t = \frac{1}{\beta} \ln(\alpha\beta) + \frac{1}{\beta} \ln t \quad (18)$$

where, α is the initial sorption rate ($\text{mg g}^{-1} \text{min}$) and β is the desorption rate constant (g mg^{-1}) during any one experiment and by assuming that $\alpha\beta t \gg 1$ [24].

5.15 Intra-particle diffusion model

During the batch mode of operation, there is a possibility of transport of sorbate species into the pores of the sorbent, which is often the rate controlling step. The rate constants of intra particle diffusion (K_{id}) at different copper ion concentrations were determined using the following linearized equation [24]:

$$Q_e = K_{id} t^{\frac{1}{2}} + D \quad (19)$$

Where Q_t is the amount of Pb(II) adsorbed at time t and $t^{1/2}$ is the square root of the time. K_{id} is the intra-particle diffusion constant ($\text{mg.g}^{-1}.\text{min}^{-1/2}$). When intra-particle diffusion plays a significant role in controlling the kinetics of the adsorption process, straight line plots through the origin are obtained and their slopes give the rate constant, k_{id} .

The slopes and intercepts of all the model curves were used to determine values of the constants as well as the equilibrium capacity (Q_e). The results indicate that the adsorption process follows only the second-order kinetic rate equation after fitting the adsorption data of Pb(II) ions onto the three activated carbon samples and the biomass (Fig. 8) and with correlation factors $R^2 = 0.9999, 0.9999, 0.9808$ and 0.9989 for CAZn, CAH, CAK and B respectively. This implies that adsorption of lead (II) ions onto the adsorbents may occur through a chemical process involving the valence forces of the shared or exchanged electrons [25]. This means that chemisorption reaction becomes more predominant in the rate-controlling step for the lead system. The straight-line plot for pseudo second order rate equation has been represented on (Fig. 8) and the values of all the model parameters and the correlation coefficients are presented in Table 5. The fact that linear plots for intra-particle diffusion model for each sample did not pass through the origin is indicative that the intra-particle diffusion was not a rate controlling step.

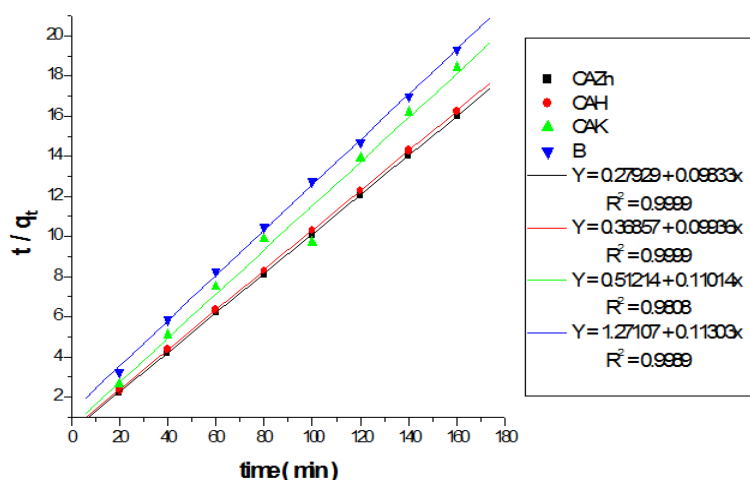


Figure 8: linearized pseudo- second order plots for Co=100mg/L, V= 50 mL, pH= 6, adsorbent dose = 0.5 g and T= 27 °C

Table 5: Results of adsorption parameters for the different kinetic models

Kinetic Models	Parameters	Adsorbents			
		CAZn	CAH	CAK	B
Pseudo-first order	Q_e (mg/g)	1.93	2.17	3.07	5.81
	K_1 (1/min)	0.0312	0.0288	0.0293	0.0320
	R^2	0.986	0.989	0.901	0.867
Pseudo-second order	Q_e (mg/g)	10.17	10.06	9.08	8.85
	K_1 (mg/g.min)	0.035	0.027	0.024	0.010
	R^2	0.9999	0.9999	0.9808	0.9989
Elovich	β (g/mg)	26.77	21.34	22.70	12.21

	α (mg/g.min)	5.23×10^5	6.84×10^3	1.71×10^3	1.76
	R^2	0.9692	0.9509	0.9621	0.9926
Intra-particle diffusion	K_{id} (mg/g.min)	0.0091	0.0113	0.0110	0.0203
	D	0.694	0.657	0.556	0.420
	R^2	0.9079	0.9051	0.9047	0.9031

VI. Conclusion

The potential of CAZn, CAH, CAK, and B as low-cost adsorbents for the uptake of Pb²⁺ ions from aqueous solutions was established. The chemical analysis by the Boehm method and the results obtained from FTIR analysis showed the presence of functional groups on the surface of the activated carbons. The equilibrium adsorption of Pb(II) ion by CAZn, CAH, CAK and B was analyzed by the Langmuir, Freundlich, Temkin and Dubinin-Radushkevich isotherm models. The Langmuir isotherm was the most appropriate model with a monolayer adsorption capacity of Pb(II) ion of 72.62 mg/g, 58.62 mg/g and 12.16 mg/g for CAZn, CAH and CAK respectively, working at pH = 6 at 27 °C. Although kinetic data for the Pb(II) adsorption were fitted to four kinetics models, namely the pseudo-first, pseudo-second-order, Elovich and intra-particle diffusion model, only the pseudo-second-order model, ($R^2 = 0.9999, 0.9999, 0.9808$ and 0.9989 for CAZn, CAH, CAK and B respectively) best described the adsorption process for all the adsorbents. From Table 6 below, it is evident that our adsorbent materials are more efficient in the sorption of Pb(II) ions than other literature studies. Hence, the present study shows that the activated carbons prepared from raphia hookeri fruit epicarps using zinc chloride and phosphoric acid as activating agent (CAZn and CAH) are effective adsorbents for the adsorption of Pb(II) ion from aqueous solution.

Table 6: Comparison of adsorption capacity of lead (II) with other adsorbents

Adsorbents	Q_{max} (mg/g)	pH	Reference
<i>militia ferruginea</i> plant leaves	3.3	4	[9]
fluted pumpkin seed shell	14.29	5	[10]
H ₃ PO ₄ treated Nipa Palm Nut (NPN)	125	5	[11]
Palm shell	1.34	5	[12]
CAZn	72.62	6	Present study
CAH	58.62	6	Present study

Acknowledgements

The authors gratefully acknowledge the support of this work by the Research Laboratory of Noxious Chemistry and Environmental Engineering of the University of Dschang.

References

- [1] U. Farooq, J. A. Farooq, M. A. Khan and M. Khan. Biosorption of heavy metal ions using wheat based biosorbents – a review of the recent literature, *Bioresource and Technology*, 101, 2010, 5043–5053.
- [2] M. Fomina and G. M. Gadd, Biosorption: current perspectives on concept, definition and application, *Bioresource Technology*. 160, 2014, 3–14.
- [3] A. Gundogdu, D. Ozdes, C. Duran, V. N. Bulut, M. Soylak, H. B. Senturk, Biosorption of Pb(II) ions from aqueous solution by pine bark (*Pinus brutia* Ten.), *Chemical Engineering Journal*, 153, 2009, 62–69.
- [4] F. J. Cerino-Cordova, P. E. Díaz-Flore, R. B. García-Reyes, E. Soto-Regalado, R. Gómez-González, and M. T. E. Bustamante-Alcántara Biosorption of Cu(II) and Pb(II) from aqueous solutions by chemically modified spent coffee grains. *International Journal of Environmental Science and Technology*. 10, 2013, 611–622.
- [5] P. Sivakumar, and P. N. Palanisamy Adsorption studies of basic Red 29 by a non-conventional activated carbon prepared from *Euphorbia ssantiqorum* L. *International Journal of Chemical Technology and Research*, 03, 2009, 502-510.
- [6] F. L. Fu, Q. Wang Removal of heavy metal ions from wastewaters: a review, *Journal of Environmental Management*, 92, 2011, 407–418.
- [7] D. M. Dragan, M. Milutin, A. Milosavljević, D. Marinković, R.Z. ĐVeljko, M. Jelena and L. B. Aleksandar, Removal of copper(II) ion from aqueous solution by high-porosity activated carbon, *NAME OF THE JOURNAL*, 39, 2013, 515- 521
- [8] K. Nasehir, E. M. Yahaya, F. P. Muhamad, L. Mohamed, I. Abustan, S. B. Olugbenga, and A. A. Mohd, Adsorptive Removal of Cu (II) Using Activated Carbon Prepared From Rice Husk by ZnCl₂ Activation and Subsequent Gasification with CO₂, *International Journal of Engineering & Technology IJET – IJENS*, 01, 2011, 164-168.
- [9] A. A. Mengistie, S. T. Silva, A. V. P. Rao and M. Singanan, Removal of lead (II) ions from aqueous solution using activated carbon from *Militia Ferruginea* plant leaves. *Bull. Chemical Society of Ethiopia*, 03, 2008, 349 - 360.
- [10] A. I. Okoye, P. M. Ejikeme and O. D. Onukwali, Lead removal from wastewater using fluted pumpkin seed shell activated carbon. Adsorption modelling and kinetics, *International Journal of Environmental Science and Technology*, 07, 2010, 793 - 800.
- [11] S. N. M. Yusoff, A. Kamari, W. P. Putra, C. F. Ishak, A. Mohamed, N. Hashim, and M. Isa, Removal of Cu(II), Pb(II) and Zn(II) Ions from Aqueous Solutions Using Selected Agricultural Wastes: Adsorption and Characterisation Studies, *Journal of Environmental Protection*. 05, 2014, 289-300.
- [12] Y. B. Onundi, A. A. Mamun, M. F. Al Khatib, and Y. M. Ahmed, Adsorption of copper, nickel and lead ions from synthetic semiconductor industrial wastewater by palm shell activated carbon, *International Journal of Engineering & Technology*, 04, 2010, 751- 758.
- [13] D. L. Ajifack, J. N. Ghogomu, J. N. Ndi, & J. M. Ketcha, Dynamics and Equilibrium studies of the adsorption of Cu(II) from aqueous solution by activated *Hibiscus Sabdariffa* L. Stalk biomass, *International Journal of Engineering Research and Technology*, 04, 2015, 655 - 664.

- [14] Kwaghger, A. and Ibrahim, J. S. (2013). Optimization of conditions for the preparation of activated carbon from mango nuts using HCl. *American Journal of Engineering Research (AJER)*, **02**, 74 - 85.
- [15] M. S. Horsfall, Equilibrium sorption study of Ag^+ , Co^{2+} , Ag^+ in aqueous solutions by fluted pumpkin (*Telfaeria Occidentalis Hook F*) waste Biomass, *Acta chimica slovinica*, **52**, 2005, 174-181.
- [16] K. Indira, Removal of methylene blue dye from aqueous solution by Neem leaf and orange peel powder, *International Journal of Chemical Technology & Research*, **05**, 2013, 572 - 577.
- [17] P. S. Kumar and K. Kirthika, Equilibrium and kinetic study of adsorption of nickel from aqueous solution onto bael tree leaf powder, *Journal of Engineering Science and Technology*, **04**, 2009, 351-363.
- [18] A. O. Dada, A. P. Olalekan, A. M. Olatunya, and O. Dada, Langmuir, Freundlich, Temkin and Dubinin-Radushkevich isotherms studies of equilibrium sorption of Zn^{2+} unto phosphoric acid modified rice husk. *IOSR Journal of Applied Chemistry (IOSR - JAC)*. ISSN: 2278 - 5736, **3**, 2012, 38 - 45.
- [19] J. N. Ndi, and M. J. Ketcha, The Adsorption Efficiency of Chemically Prepared Activated Carbon from Cola Nut Shells by ZnCl_2 on Methylene Blue, *Journal of Chemistry*, **2013**, 2013, 1-7
- [20] J. N. Ghogomu, T. D. Noufame, M. J. Ketcha and N. J. Ndi, Removal of Pb(II) ions from Aqueous Solutions by Kaolinite and Metakaolinite materials, *British Journal of Applied Science and Technology*, **04**, 2013, 942-961.
- [21] Y. S. Ho, C. T. Huang, and H. W. Huang, Equilibrium sorption isotherm for metal ions on tree fern, *Process Biochemistry*, **37**, 2002, 1421 - 1430.
- [22] C. Y. Abasi, A. A. Abia, and J. C. Igwe, Adsorption of Iron (III), Lead (II) and Cadmium (II) ions by unmodified Raphia Palm (*Raphia hookeri*) Fruit Endocarp, *Environmenta. Research. Journal*, **05**, 2011, 104 - 113.
- [23] S. T. Abbas, Isotherm, kinetics and thermodynamics of Adsorption of heavy metal ions onto local activated carbon. *Aquatic science and Technology*, **01**, 2013, 53 - 77.
- [24] M. A. Abuh, G. K. Akpomie, N. K. Nwagbara, N., Abia-Bassey D. I. Ape, and B. U. Ayabie, Kinetic rate equation: Application on the removal of copper (II) and zinc (II) by unmodified Lignocellulosic fibrous layer of palm tree trunk- single component system studies, *International Journal of Basic and Applied Science*, **04**, 2013, 801 - 809.
- [25] S. Wang, and H. Li, Kinetic modelling and mechanism of dye adsorption on unburned carbon, *Dyes Pigments*, **72 (3)**, 2007, 308-314.